Redesigning Kinase Inhibitors to Enhance Specificity

Alejandro Crespo,[†] Xi Zhang,[‡] and Ariel Fernández*,[†]

Department of Bioengineering, Rice University, Houston, Texas 77005, Program in Applied Physics, Rice Quantum Institute, Rice University, Houston, Texas 77005

Received April 21, 2008

Kinases are important targets in molecular cancer therapy. However, the evolutionary relatedness and structural conservation of these proteins often lead to unforeseen cross reactivity, yielding unexpected side effects. Thus, the use of promiscuous drugs is likely to introduce dangerous clinical uncertainties. Here, we show how to rationally redesign two promiscuous kinase inhibitors, staurosporine (**7**) and EKB-569 (**8**), with the goal of turning them into more selective ligands. This problem is addressed by exploiting a structure-based selectivity filter for specificity: the pattern of packing defects in the target. These singularities, called *dehydrons*, are solvent-exposed intramolecular hydrogen bonds that may be protected by drugs upon association and are *not* conserved across protein families. Our redesigned compounds possess a significantly focused activity, as experimentally corroborated in high-throughput screening assays. Thus, our design strategy proves to be operative to reduce the inhibitory impact of promiscuous kinase ligands, enhancing their safety as therapeutic agents.

Introduction

The use of small-molecule inhibitors of protein function is one of the most efficient ways to treat human disease and malignancy.[1–5] In this regard, protein kinases, the essential signal transducers, have become important targets in molecular cancer therapy.[1–5] However, most protein targets of therapeutic interest have surviving paralogues, i.e., proteins that share a common ancestor with the target and have diverged after speciation.[6] In particular, kinases are lumped up into families, which typically share a very similar fold and specific structural features.[6,7] This structural conservation is often responsible of unexpected cross reactivities,[8,9] yielding uncertain or even life-threatening side effects.[10–12]

Although there is no clear correlation between anticancer activity and specificity, promiscuous inhibitors are obviously more prone to yield side effects than selective drugs. Even the most successful anticancer drug imatinib (STI571, **1**),[3,13] with an activity profile limited to 5 primary kinases (Abl, C-Kit, Lck, PDGFR, and CSF1R),[8,9] has shown to be potentially cardiotoxic.[11,12] Moreover, the more promiscuous anticancer kinase inhibitors[8,9] sunitinib (SU11248, **2**)[14] and sorafenib (Bay 43-9006, **3**)[15] have also been found to be cardiotoxic, and to an even larger extent than imatinib.[12] The other commercial kinase inhibitors (Scheme 1) dasatinib (BMS-354825, **4**),[16] erlotinib (OSI-774, **5**),[17] and gefitinib (ZD1839, **6**)[18] have also a broad activity profile.[8,9]

The therapeutic use of promiscuous inhibitors may be potentially hazardous unless a rational strategy to control their specificity is adopted. Such control may be achieved if we can identify selectivity filters in the target, i.e., structural features that are unique to the target, and chemical modifications to the drug that promote interactions with such unique features. Thus, much of the cross reactivity may be removed by redesign guided by the identification of structural features that promote promiscuity and selectivity filters that enable target discrimination.[19–22]

A selectivity filter of broad applicability has been recently identified: the packing defects of soluble proteins.[23–27] These defects consist of solvent-exposed intramolecular backbone hydrogen bonds and constitute vulnerabilities arising from imperfections in side chain packing. These structural singularities, called dehydrons,[25] are targetable-sticky spots because they promote their own further dehydration as a means to strengthen and stabilize the underlying amide-carbonyl electrostatic interaction.[23–27] Dehydrons have been turned into an operational selectivity filter for two reasons: (i) they may be targeted by drugs that further wrap them (protect from water attack) by bringing nonpolar groups to their proximity upon association[19,28,29] and (ii) they are not conserved across paralogues.[6,30] In this work, we report on a rational redesign of promiscuous inhibitors to exogenously wrap nonconserved dehydrons with the goal of enhancing their target-discriminatory power.

In principle, most kinase inhibitors can be turned into selective wrappers of dehydrons through minimal chemical modification that preserve the generic chemotype. Thus, relevant kinase inhibitors with considerable cross reactivities such as staurosporine (**7**)[31] (inhibiting 87% out of the 290 kinases screened with $K_D < 3\ \mu M$),[9] sunitinib (57%), dasatinib (28%), EKB-569 (**8**)[32] (18%), sorafenib (18%), erlotinib (15%), gefitinib (7%), or imatinib (6%) may in principle be turned into drugs with enhanced specificity through wrapping redesign. The generic strategy consists of modifying the parental compound to turn it into a wrapper of unique dehydrons while also removing potential sources of cross reactivity. These arise because ligand groups are often engaged in interactions with groups on the backbone or on side chains that are invariant across the target family.

To test the target-discriminatory power of wrapping redesign, we focus in this work on a major challenge arising thereof: the re-engineering of promiscuous inhibitors. First, we report on the redesign of staurosporine (Scheme 2), the most promiscuous kinase inhibitor known,[9] to elicit an inhibitory impact with enhanced specificity. Our redesign introduces a single wrapping modification to target one of the least conserved kinase dehydrons. The resulting ligand **9** (Scheme 2) possesses a significantly more focused impact than the parental compound, as corroborated in high-throughput screening assays. We also report on the successful cleaning of the "dirty" inhibitor **8**

* To whom correspondence should be addressed. Phone: (713)348-3681. Fax: (713)348-3699. E-mail: arifer@rice.edu.
[†] Department of Bioengineering, Rice University.
[‡] Program in Applied Physics, Rice Quantum Institute, Rice University.

10.1021/jm800453a CCC: $40.75
Published on Web 08/05/2008

Scheme 1. Chemical Structures of Commercial Anticancer Drugs

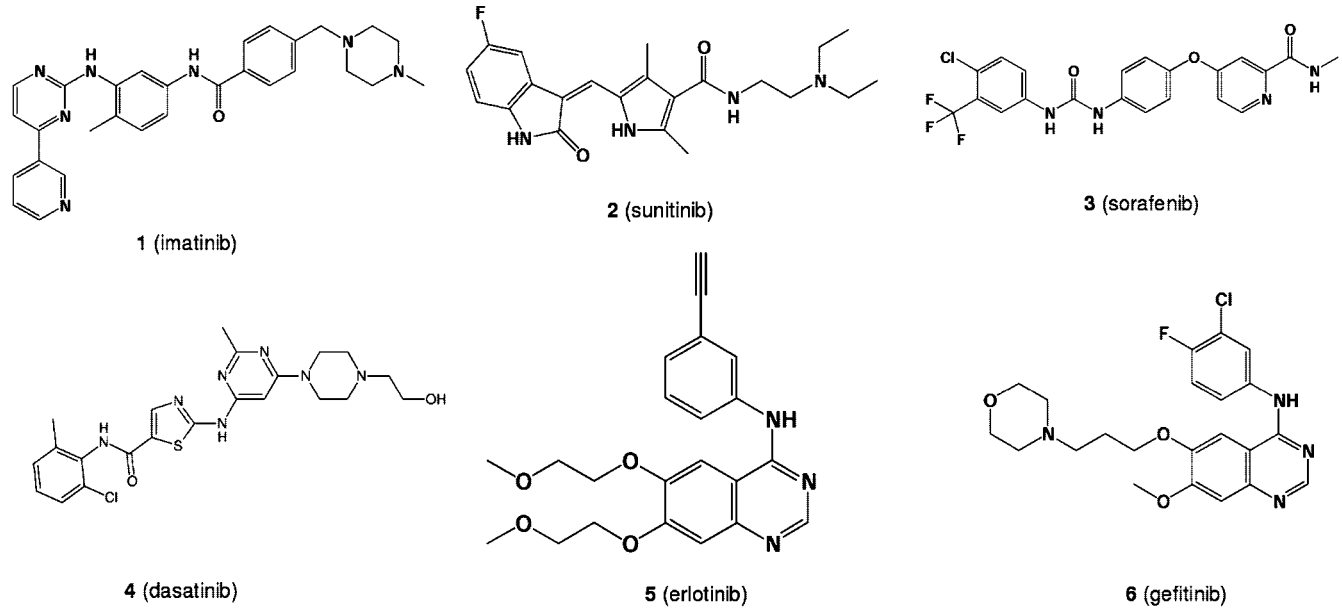

Scheme 2. Chemical Structures of Compounds **7** and **9**

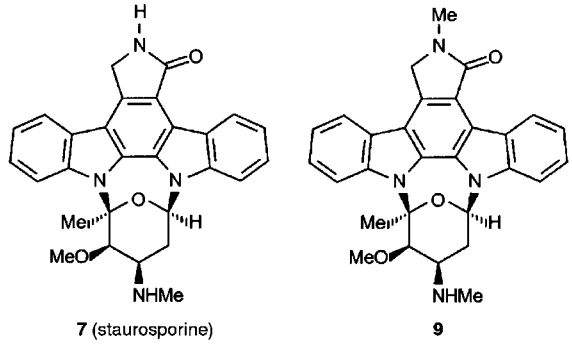

Scheme 3. Chemical Structures of Compounds **8** and **10**

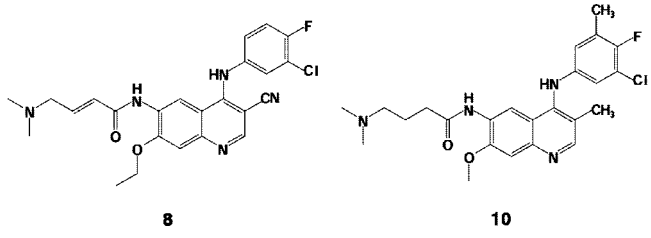

(Scheme 3). This is carried out by removing the promiscuity-promoting elements in the compound while appending a nonpolar group that wraps a unique dehydron of the primary target of **8**, the epidermal growth factor receptor (EGFR) kinase. The experimental high-throughput screening assay of the wrapping compound **10** (Scheme 3) confirms its considerably focused activity profile.

The solution to the challenging design problems presented in this work singles out the wrapping redesign as a paradigm shifter in the engineering of highly selective inhibitors.

Results

Staurosporine Redesign. Staurosporine is the most cross-reactive kinase inhibitor known to date.[8,9] It binds tightly (K_D < 3 μM) to ~90% of the 119 (or 290 in the latest assay) human kinases screened through phage-display ATP-competitive assays.[8,9] Such levels of cross reactivity make it impossible to envision staurosporine as a therapeutic agent. Thus, despite its inhibitory potency, staurosporine is solely regarded as a research compound.[8,9] Staurosporine is a natural competitive inhibitor that binds to the ATP pocket of almost all kinases in the active conformation (the activation loop is fully extended and exposed to solvent).[33–35] To illustrate its binding mode, the crystal structure of the EGFR kinase in complex with staurosporine is shown in Figure 1 (PDB 2ITW). Staurosporine has a larger solvent-accessible surface area than ATP (360 Å^2 vs 323 Å^2, respectively),[36] and it is a more rigid molecule, hence reducing the entropic penalty upon association. The high promiscuity of this inhibitor is due to the numerous contacts it makes (it is a

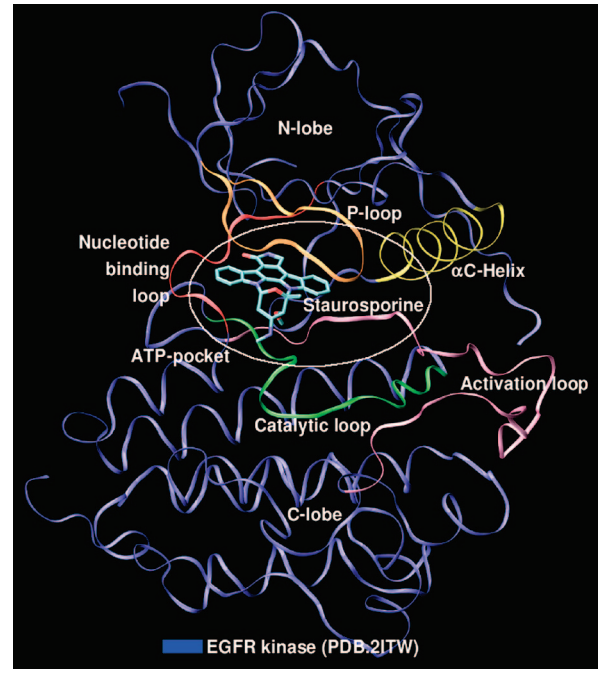

Figure 1. Ribbon representation of EGFR kinase (PDB 2ITW, blue) in complex with staurosporine. Relevant structural features that frame the ATP-pocket (white circle) are depicted for clarity: nucleotide-binding loop (red), P-loop (orange), αC-helix (yellow), catalytic loop (green), and activation loop (pink).

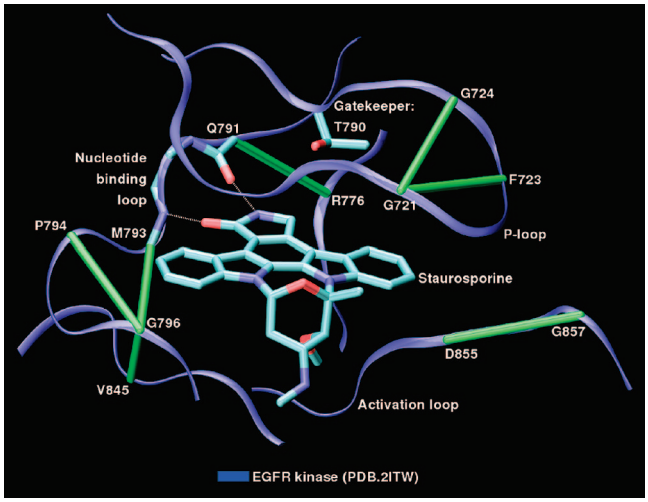

Figure 2. Induced-fit conformation of the ATP-binding pocket of EGFR kinase (PDB 2ITW, blue) generated when crystallized with staurosporine. The ligand forms two hydrogen bonds with the conserved backbone atoms of residues in the nucleotide-binding loop (Q791 and M793) and hydrophobic interactions with residues framing the pocket (gatekeeper: T790). EGFR kinase has seven dehydrons (green virtual bond joining α-carbons) within its binding pocket: G721-F723 and G721-G724 in the P-loop, R776-Q791, M793-G796, P794-G796, and G796-V845 in the nucleotide-binding loop, and D855-G857 in the activation loop.

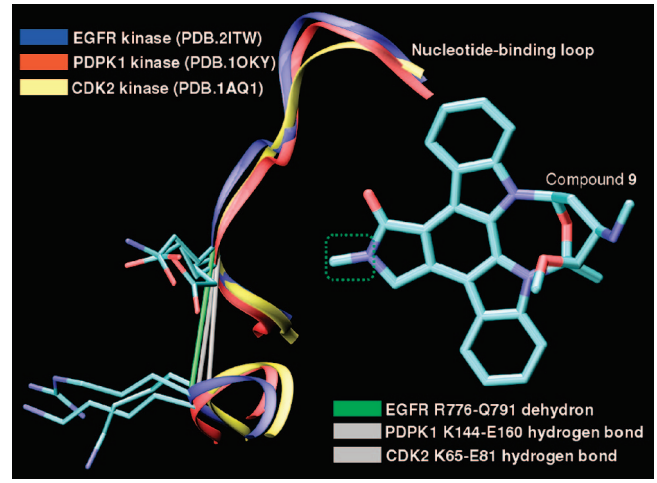

Figure 3. Selected aligned backbones (ribbon representation) of EGFR (PDB 2ITW, blue), PDPK1 (PDB 1OKY, red), and CDK2 (PDB 1AQ1, yellow) kinases complexed with compound **9**. The R776-Q791 dehydron in EGFR (green virtual bond joining α-carbons) maps into the well-wrapped backbone hydrogen bonds (gray virtual bonds joining α-carbons) K144−E160 in PDPK1 and K65-E81 in CDK2. The methyl group at the pyrrol N6-position (indicated by the green box) turns the ligand into a wrapper of the nonconserved dehydron.

large and rigid nonpolar molecule) with conserved polar and hydrophobic groups of protein kinases.[33–35] For example, it makes strong van der Waals interactions with residues framing the ATP pocket such as L718, G719, F723, V726, A743, K745, T790, L792, M793, G796, S797, and L844. Staurosporine also forms two hydrogen bonds with the conserved backbone atoms of residues in the nucleotide-binding loop: Q791:*O*-Pyrrol:N6 and M793:*N*-Pyrrol:O5 (Figure 2). These residues are also involved in intermolecular hydrogen bonds with ATP. These extensive interactions with conserved regions make the re-engineering of staurosporine a challenging problem.

To redesign staurosporine through a wrapping modification, we compare all 37 PDB structures of kinases in complex with ligands that share the same indolo[2,3-*a*]pyrrolo[3,4-*c*]-carbazole chemotype (Methods). The EGFR-staurosporine complex has seven dehydrons within the ATP pocket: G721-F723 and G721-G724 in the P-loop, R776-Q791, M793-G796, P794-G796, and G796-V845 in the nucleotide-binding loop, and D855-G857 in the activation loop (Figure 2). From these seven, dehydrons R776-Q791, M793-G796, and D855-G857 are potentially more accessible to a wrapping modification of staurosporine (at least one α-carbon of the residues paired by the dehydron is within 7 Å from any atom of the ligand). A comparative wrapping analysis of the 37 aligned structures reveals that dehydron R776-Q791 is the least conserved and more easily accessible to a wrapping modification (generally methylation) in this structural assortment. This dehydron is conserved in 8 out of the 37 kinase structures, ABL1, EGFR, GSK3β, LCK, MAP3K5, MAP3K17, PTK2, and SRC (Figure 3, Table 1), whereas dehydrons M793-G796 and D855-G857 are conserved in 9 and 12 structures, respectively. Thus, dehydron R776-Q791 may be targeted by wrapping it through a specific methylation of staurosporine (compound **9**) at the imide N6-position of the pyrrol ring (Figure 3, Methods).[31,33,37] This modification is mostly useful because will also remove one conserved hydrogen-bond interaction, increasing specificity. Thus, by redesigning staurosporine to turn it into a wrapper of the R776-Q791 dehydron in EGFR, we can significantly restrict its inhibitory impact to the 8 kinases that share the dehydron at the aligned position (Table 1). The bacteriophage high-throughput screening of **9** is shown in Figure 4: *only 26 kinases representing 12% of the 220 kinases assayed have significant affinity for the ligand. This percentage hit signals a massive enhancement in selectivity when compared with the 88% of the parental compound.* Most significantly, our structure-based prediction of affinity based on the presence or absence of the dehydron at the aligned position includes five hits (ABL1, EGFR, LCK, PTK2, and SRC), only one false positive (MAP3K5) and not a single false negative over the 18 instances (Table 1) where packing prediction can be contrasted with experiment. These results reveal ~94% of accuracy in the prediction. The other hits of **9** are: AAK1, ABL1 (H396P), ABL1 (T315I), ABL1 (Y253F), CAMK2A, CAMK2B, CAMK2D, CAMK2G, CAMKK1, CAMKK2, CSF1R, FLT3, KIT, KIT (D816V), LOK, MARK2, PAK6, PDGFRA, PDGFRB, PTK2B, and SLK. For these cases, we either do not have a crystal structure of the protein or the protein is crystallized in complex with a ligand other than staurosporine and hence with a different induced fit. However, all these hits correspond to staurosporine targets with high-binding affinity (nM or sub-nM range).[9] In cases of PDB-reported structure with a ligand other than staurosporine, wrapping predictions can be made but without the same confidence. For example, the active KIT structure complexed with ADP (PDB 1PKG) has a dehydron at the aligned position. Thus, all close KIT paralogues (CSF1R, FLT3, PDGFRA, PDGFRB with sequence identity >60%) will probably be targeted by **9**, as corroborated in the screening (Figure 4). Furthermore, the LOK kinase (PDB 2J7T) has a dehydron in such position and represents a hit. However, PAK6 (PDB 2C30) and SLK (PDB 2J51) have a well-wrapped hydrogen bond, and **9** still binds. Therefore, affinity predictions based on structures crystallized with ligands other than staurosporine are less reliable. However, the accuracy of our prediction is still high (46 out of 56 cases or ~82%) if we further extend our structure-based analysis to include the set of 53 kinases with reported PDB structure that were recently screened (Methods)[8] (Table S1, Supporting Information). Nevertheless, the higher selectivity of **9** is significant, showing high in vitro activity

Table 1. Wrapping Comparison of the 37 PDB-Reported Kinases in Complex with Staurosporine or with Ligands that Share the Same Chemotype at Position Aligned with EGFR Dehydron R776-Q791 (DH = Dehydron, HB = Well-Wrapped Hydrogen Bond)[a]

kinase	PDB	wrapping classification	hit in screening	match prediction experiment
ABL1	2HZ4	DH	HIT	YES
CDK2	1AQ1	HB	NO HIT	YES
CHK1	1NVR	HB	not screened	
DAPK1	1WVY	HB	not screened	
EGFR (WT)	2ITW	DH	HIT	YES
EGFR (G719S)	2ITQ	HB	not screened	
EGFR (L858R)	2ITU	HB	not screened	
FYN	2DQ7	HB	NO HIT	YES
GSK3β	1Q3D	DH	not screened	
IRAK4	2NRY 2OIC	HB	not screened	
ITK	1SM2 1SNU	HB	NO HIT	YES
JAK3	1YVJ	HB	not screened	
LCK	1QPD 1QPJ	DH HB	HIT	YES
MAP3K5	2CLQ	DH	NO HIT	NO
MAP3K17	2GCD	DH	not screened	
MAPKAPK2	1NXK 2PZY	HB	not screened	
MET	1R0P	NO HB	NO HIT	YES
MKNK2	2HW7	HB	NO HIT	YES
PAK1	2HY8	HB	NO HIT	YES
PDPK1	1OKY 1OKZ	HB	NO HIT	YES
PIK3CG	1E8Z	HB	not screened	
PIM1	1YHS	HB	NO HIT	YES
PIM2	2IWI	HB	NO HIT	YES
PKAC-α	1STC	HB	NO HIT	YES
PRKCQ	1XJD	HB	not screened	
	2J0J	HB		
PTK2	2J0K	DH	HIT	YES
	2J0M	DH		
SRC	1BYG	DH	HIT	YES
STK16	2BUJ	NO HB	not screened	
SYK	1XBC	HB	NO HIT	YES
ZAP70	1U59	HB	NO HIT	YES

[a] Compound **9** is predicted to bind only to kinases that have a dehydron at the aligned position, and the prediction is contrasted with its experimental screening.

toward selected therapeutically relevant targets such as KIT (for treatment of gastrointestinal stromal tumors),[38] PTK2 (involved in the metastasis of ovarian carcinoma),[39] SRC (implicated in the metastatic/invasive phenotype),[40] or EGFR (for treatment of nonsmall cell lung cancer).[41,42] Thus, the wrapping modification of staurosporine may potentially be turned into a realistic clinical opportunity.

Cleaning Inhibitor 8. The irreversible kinase inhibitor **8** developed by Wyeth-Ayerst[41] was launched as a major inhibitor of the EGFR kinase (IC_{50} = 38.5 nM). Thus, its therapeutic interest to treat nonsmall cell lung cancer (NSCLC), colorectal neoplasia, and other EGFR-dependent solid tumors became apparent.[41,42] Phase I and II trials for such therapeutic applications are currently in progress and closed to new patients.[42] Recent high-throughput screening assays[8,9] revealed ~50 targets (K_D < 3 μM) for **8**, making it a promiscuous drug with likely side effects. Other anti-NSCLC agents such as gefitinib or erlotinib share the same 4-anilinoquinoline chemotype,[32] yet they are more specific EGFR inhibitors.[8,9]

The promiscuity of **8** can be traced to its intermolecular interactions with highly conserved residues within the EGFR kinase family. Compound **8** has a large solvent-accessible surface area (397 Å^2)[36] that may increase the nonspecific van der Waals interactions with residues framing the ATP pocket. Moreover, its polar amide group that increases drug solubility may be involved in hydrogen bonds with backbone atoms of residues in the P-loop or in the nucleotide-binding loop. As shown in Figure 5, one important source of promiscuity of compound **8** is its terminal acryl group, which plays the role of electrophile in the irreversible Michael reaction with the nucleophile-conserved residues Cys or Ser in the nucleotide-binding loop of EGFR paralogues. The water-solublizing terminal *N*-dimethyl group may also accelerate such addition, serving as an intramolecular base catalyst for Michael reaction with the Cys or Ser residues due to the spatial proximity.[32] Another source of promiscuity of compound **8** is the intermolecular electrostatic interaction between its cyanide group and the gatekeeper residue (Thr or Met), typically conserved within the family (Figure 5).

To validate whether such interactions are responsible for the promiscuity of compound **8**, we establish a correlation between the affinities of **8** for 53 paralogues of EGFR reported in the PDB (Methods) and the extent of residue conservation at the Michael reaction site and at the gatekeeper position. To do so, we align each paralogue structure with the EGFR structure (PDB 1M17) and examine residues that align with C797 (Michael reactant) and T790 (gatekeeper) (Methods).[43,44] A statistical model is built to assess such correlation (Methods),[45,46] revealing that the affinity profile of **8** is indeed dictated by these two sources of promiscuity (*P*-value = 0.007). Thus, the terminal acryl group and the cyanide group of **8** (Figure 5) are the "dirty" moieties responsible for its promiscuity.

We thus remove the sources of promiscuity by introducing the two following chemical modifications (Figure 6): (i) Replace the double bond (the Michael acceptor) in the acryl group with a single bond. (ii) Replace the cyanide group with a methyl to retain the chemotype while removing the electrostatic interaction with the gatekeeper.

To promote selectivity, we further introduce a wrapping modification in the drug to target a nonconserved dehydron in the intended target. When EGFR is crystallized in the induced-fit conformation generated by an inhibitor (erlotinib) that shares **8′**s 4-anilinoquinoline chemotype (PDB 1M17), we now find only six dehydrons within the binding pocket (Methods): G721-F723 and G721-G724 in the P-loop, M793-G796, P794-G796, and G796-V845 in the nucleotide-binding loop, and D855-G857 in the activation loop. From these six, dehydrons M793-G796 and D855-G857 are potentially more accessible to a wrapping modification of the drug. By examining these two dehydrons across the 53 EGFR-paralogues, we find that the least conserved and more accessible to a wrapping modification is dehydron D855-G857 (Figure 6). Only 12 paralogues retain this dehydron (Table 2): AURKA, CLK3, EGFR, EPHA3, ERBB2, FYN, LCK, PAK6, PAK7/PAK5, PIM2, SLK, and STK10, whereas dehydron M793-G796 is conserved in 17 kinases. Thus, we choose dehydron D855-G857 as the nonconserved selectivity feature to be targeted. To do so, we append a methyl group at position 3 of the terminal benzene ring of **8** that becomes a wrapper or protector of such feature (Figure 6). The synthesis of the redesigned compound **10** follows a pathway that recapitulates the synthesis of the parental compound **8** (Methods).[32] Compound **10** buries a solvent-accessible surface area similar to **8′**s (393 Å^2 vs 397 Å^2, respectively),[36] showing a similar size and binding orientation and similar entropic penalty upon association. However, **10** not only lacks **8′**s sources of promiscuity but also introduces a wrapping modification to promote selectivity.

Our structure-based affinity profile prediction for **10** is based on the conservation of the EGFR D855-G857 dehydron wrapped

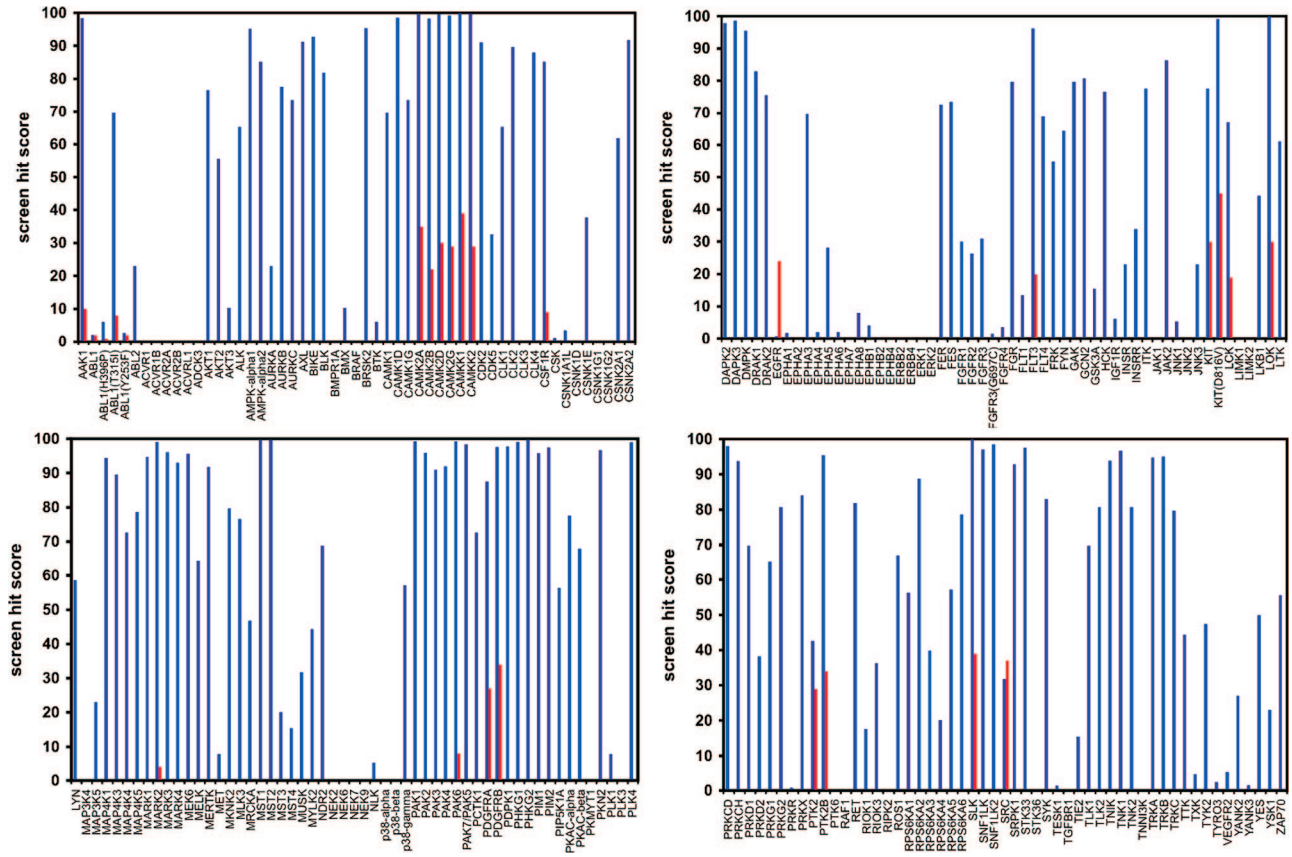

Figure 4. Affinity profile of compound **9**. High-throughput screening at 10 μM of **9** (red) over a battery of 220 human kinases displayed in a T7-bacteriophage-expressing library (Ambit Bioscience, San Diego, CA). The screening assay of staurosporine (blue) was used as control.[8,9] Hit values are reported as percentage bound kinase.

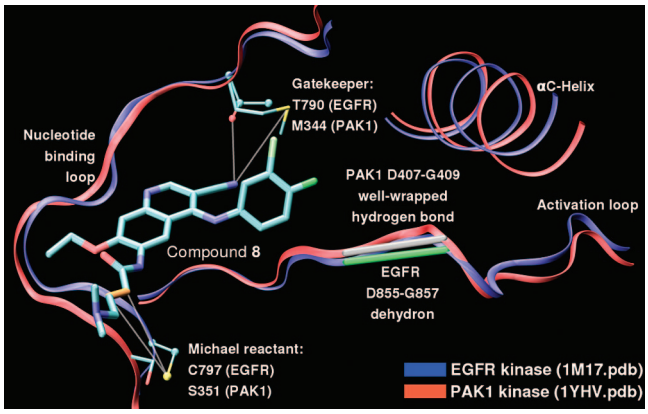

Figure 5. Structural alignment of two targets of **8**: the EGFR kinase (PDB 1M17, blue ribbon representation, atoms in balls and sticks) and the paralogue PAK1 kinase (PDB 1YHV, red ribbon representation, atoms licorice), complexed with the drug (licorice). Atoms are depicted following standard color convention (chlorine in green, fluorine in light green). The sources of promiscuity of compound **8** are the terminal acryl group (electrophile group in the Michael reaction) and its cyanide group (involved in intermolecular electrostatic interaction with a Thr or Met gatekeeper). EGFR has a poorly conserved D855-G857 dehydron (green virtual bond joining α-carbons) that may be targeted to achieve selectivity. PAK1 contains the same two promiscuity-fostering features, while it has a well-wrapped hydrogen bond aligned at such position (gray virtual bond joining α-carbons). Targeting such dehydron will ensure a discriminatory binding of EGFR without hitting PAK1, as experimentally corroborated.

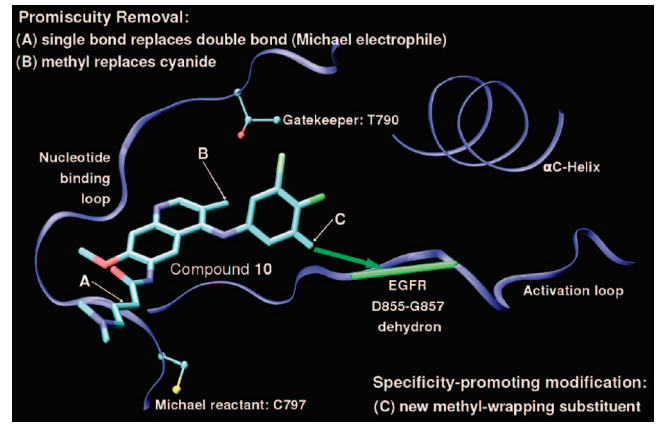

Figure 6. EGFR kinase structure (same representation as Figure 5) complexed with compound **10** (licorice representation). To remove promiscuity, the acrylic double bond (Michael electrophile) and the gatekeeper-interacting cyanide group of **8** are replaced by a single bond and a methyl group, respectively. To selectively target EGFR, another methyl group is added to the terminal benzene ring as a wrapper of the least conserved D855-G857 dehydron (green virtual bond joining α-carbons).

by **10** (*but not by* **8**) and the existence of steric hindrances with the targets. In cases where there is a dehydron aligned with the EGFR D855-G857 dehydron, we predict steric hindrance only for those kinases that originally do not bind to **8** because they are likely to also clash sterically with **10**. This is expected because the binding to **8** implies that no steric hindrance occurs (the reciprocal does not hold). *We thus predict as "hits" only those kinases that introduce no steric hindrance and possess a dehydron in the position that aligns with EGFR D855-G857.* Only 8 hits are thus predicted (Table 2): CLK3, EGFR, EPHA3, ERBB2, FYN, LCK, SLK, and STK10. In cases where the residues aligning with EGFR D855-G857 are not engaged in a

Scheme 4. Synthetic Pathway of Compound **10**[a]

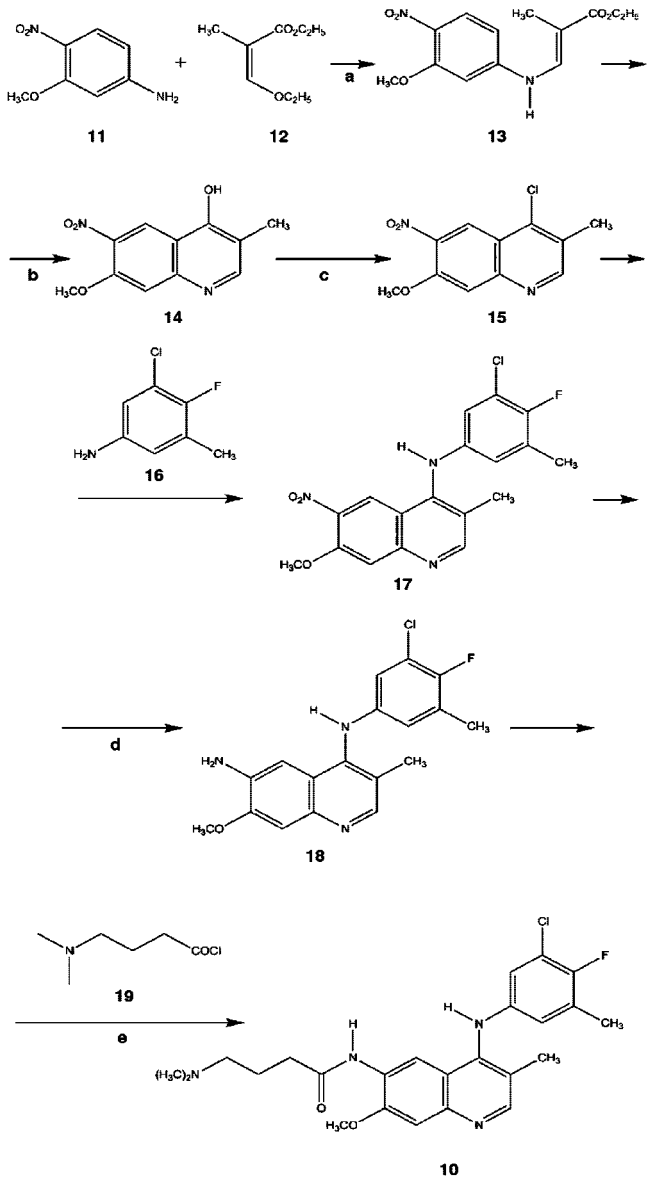

[a] (a) Toluene, reflux. (b) Dowtherm, 256 °C. (c) $POCl_3$, reflux. (d) Fe, NH_4Cl, CH_3OH, reflux. (e) *N,N*-diisopropylethylamine, THF, 0 °C. See *Supporting Information* for details.

dehydron or in a well-wrapped hydrogen bond, we further examine whether such a dehydron can be induced upon ligand binding with a minimal structural adaptation. Four kinases (ABL1 (H396P), BTK, PTK2, and SYK, out of 6 cases: ABL1 (H396P), BTK, FLT3, PTK2, STK16, and SYK) can induce this dehydron upon drug binding with no steric hindrance, representing "possible" hits (Table 2). *The experimentally obtained affinity profile (Table 2*, Figure 7) for compound **10** *agrees very well with our predicted profile: it actually binds 6 (CLK3, EGFR, ERBB2, LCK, SLK, and STK10) out of the 8 hits inferred with certainty and two of the possible hits (BLK and PTK2).* It has only 3 false positives (EPHA3, FYN, and the other possible hit SYK) and not a single false negative (Table 2) for the 50 cases where our prediction can be contrasted with experiment. These results show ~94% of accuracy in the prediction.

These results reveal that the wrapping redesign introduces a significant increase in the selectivity of the "dirty" inhibitor **8**. This is accomplished by first removing the drug features that promote promiscuity. Subsequently, we introduce a chemical modification that wraps a relatively unique dehydron in the intended kinase target. This rational redesign makes compound **10** more selective than the parental compound **8**: out of the 220 kinases experimentally screened, compound **10** binds strongly (sub-μM affinity or % of inhibition >10) to 5 kinases, whereas compound **8** binds to 19 (Figure 7).

Conclusions

This work describes and validates a generic strategy in molecular design aimed at turning highly cross-reactive kinase inhibitors into significantly more selective drugs. To demonstrate the power of this approach, we selected the most challenging design problems, represented by the cleaning of the highly promiscuous ligands staurosporine and inhibitor **8**. The redesign of these compounds was guided by a selectivity filter: the pattern of packing defects, the so-called *dehydrons*, in the drug target that are not conserved across paralogues.[25,30] Thus, relatively unique dehydrons have been targeted by the redesigned compounds to further protect them from water attack upon association. In this way, we have significantly enhanced specificity in a highly controllable manner and even for the most promiscuous kinase inhibitors. Thus, a generic strategy may involve modifying the parental compound to turn it into a wrapper of poorly conserved dehydrons while removing potential sources of ligand promiscuity. This strategy may be successfully applied to other cross-reactive kinase inhibitors such as sunitinib and sorafenib, documented to entail a risk of side effects.[12] The structure-based affinity predictions for our wrapping prototypes were benchmarked against experimental screening,[8,9] revealing over 90% accuracy. The reliability of wrapping predictions is contingent on the availability of target structures. The latter are typically reported for induced-fit conformations arising in drug/target complexes. Hence, the wrapping prediction requires that the PDB-reported complexes share the same ligand chemotype as the parental compound to ensure induced-fit similarity. Particular attention to induced-fit diversity is needed in drug design, especially in wrapping design, due to the conformational plasticity of kinases. Thus, wrapping design will undoubtedly benefit from an ever-increasing amount of reported data on structural adaptation of targets to diverse ligands as well as high-throughput screening of drug variants, enabling a dissection of specificity-promoting features. The efficacious solution to the problem of cleaning promiscuous drugs reported here highlights the value of the wrapping redesign as a paradigm shifter in the engineering of drug selectivity.

Methods

Target Identification. To redesign staurosporine performing a comparative analysis of nonconserved selectivity features, we collected all 37 PDB-reported kinase structures complexed with staurosporine or with ligands that share the same indolo[2,3-*a*]pyrrolo[3,4-*c*]-carbazole chemotype.[37] We only selected kinase structures in complex with such ligands, to avoid a less reliable identification of dehydrons, arising from different induced fits generated in presence of other drug/inhibitors.

A similar structural analysis was performed for cleaning **8**. Because its primary intended target is the EGFR kinase, we adopted a PDB-reported structure of EGFR in complex with an inhibitor (erlotinib) that shares the same 4-anilinoquinoline chemotype (PDB 1M17).[32] A comparative analysis to identify potential sources of cross reactivity and nonconserved specificity-promoting features was performed for the 53 EGFR-paralogues with reported PDB structure that were recently screening using a battery of 119 T7-phage expressed kinases.[8]

Table 2. Wrapping Comparison for the Set of 53 Paralogue Kinases of EGFR with Reported PDB Structure[a]

kinase	PDB	wrapping classification	steric hindrance	predicted affinity	experimental affinity	match prediction experiment
ABL1	2GQG			NO HIT	NO HIT	YES
ABL1 (T315I)	2V7A			NO HIT	not screened	
ABL1 (H396P)	2F4J	possibly induced	NO	possible HIT	not screened	
AURKA	1MQ4	DH	YES	NO HIT	NO HIT	YES
BTK	1K2P	possibly induced	NO	possible HIT	HIT	YES
CAMK1D	2JC6			NO HIT	NO HIT	YES
CAMK1G	2JAM			NO HIT	NO HIT	YES
CDK2	1AQ1			NO HIT	NO HIT	YES
CDK5	1UNG			NO HIT	NO HIT	YES
CLK1	1Z57			NO HIT	NO HIT	YES
CLK3	2EU9	DH	NO	HIT	HIT	YES
CNSK1G1	2CMW			NO HIT	NO HIT	YES
CNSK1G2	2C47			NO HIT	NO HIT	YES
DAPK2	2A2A			NO HIT	NO HIT	YES
DAPK3	2J90			NO HIT	NO HIT	YES
EGFR	1M17	DH	NO	HIT	HIT	YES
EPHA2	1MQB			NO HIT	NO HIT	YES
EPHA3	2QO9	DH	NO	HIT	NO HIT	NO
ERBB2	1OVC	DH	NO	HIT	HIT	YES
FGFR1	1AGW			NO HIT	NO HIT	YES
FGFR2	1GJO			NO HIT	NO HIT	YES
FLT3	1RJB	possibly induced	YES	NO HIT	NO HIT	YES
FYN	2DQ7	DH	NO	HIT	NO HIT	NO
HCK	1QCF			NO HIT	NO HIT	YES
INSR	1GAG			NO HIT	NO HIT	YES
JAK2	2B7A			NO HIT	NO HIT	YES
JNK1	1UKH			NO HIT	NO HIT	YES
JNK3	1PMN			NO HIT	NO HIT	YES
KIT	1PKG			NO HIT	NO HIT	YES
LCK	1QPC	DH	NO	HIT	HIT	YES
MAP3K5	2CLQ			NO HIT	NO HIT	YES
MKNK2	2AC3			NO HIT	NO HIT	YES
NEK2	2JAV			NO HIT	NO HIT	YES
P38-α	1DI9			NO HIT	NO HIT	YES
P38-γ	1CM8			NO HIT	NO HIT	YES
PAK1	1YHV			NO HIT	NO HIT	YES
PAK4	2CDZ			NO HIT	NO HIT	YES
PAK6	2C30	DH	YES	NO HIT	NO HIT	YES
PAK7/PAK5	2F57	DH	YES	NO HIT	NO HIT	YES
PDGFRB	1LWP			NO HIT	NO HIT	YES
PIM1	1YXT			NO HIT	NO HIT	YES
PIM2	2IWI	DH	YES	NO HIT	NO HIT	YES
PKAC-α	2GU8			NO HIT	NO HIT	YES
PTK2	2ETM	possibly induced	NO	HIT	HIT	YES
RPS6KA5	1VZO			NO HIT	NO HIT	YES
SLK	2J51	DH	NO	HIT	HIT	YES
SRC	2SRC			NO HIT	NO HIT	YES
STK10	2J7T	DH	NO	HIT	HIT	YES
STK16	2BUJ	possibly induced	YES	NO HIT	not screened	
SYK	1XBB	possibly induced	NO	possible HIT	NO HIT	NO
TIE2	1FVR			NO HIT	NO HIT	YES
TNK2	1U46			NO HIT	NO HIT	YES
VEGFR2	2P2H			NO HIT	NO HIT	YES

[a] Compound **10** is predicted to bind only to kinases with a dehydron or possibly induced dehydron in positions aligning with EGFR D855-G857 dehydron and with no steric hindrance. The prediction is contrasted with its experimental screening.

Moreover, the comparative wrapping analysis for staurosporine redesign was further extended to include this set of 53 paralogue kinases with reported PDB structure (Supporting Information).

For such comparative analysis, we have performed a structural alignment of all kinases in each set of targets. The alignment was performed using the DaliLite web-based program for pairwise structure comparison.[43,44] Structure conservation across targets within kinase families enables such alignment.[6]

Statistical Analysis. To verify that the sources of promiscuity of compound **8** are the extent of residue conservation at both the Michael reaction site and at the gatekeeper position, we performed a statistical analysis by building a logistic regression model.[45,46] Thus, we established a correlation between the affinities of **8** for the set of 53 EGFR-paralogues reported in PDB and the extent of residue conservation at such positions. The two "explanatory variables" are the types of residues aligning with C797 (Michael nucleophile) and T790 (gatekeeper). Thus, $X_1 = 1$, if the residue aligning with C797 is Cys or Ser (possible Michael nucleophiles), and $X_2 = 1$, if the residue aligning with T790 is Thr or Met (possible intermolecular electrostatic interaction with the cyanide group). The "responding variable" is the affinity of **8** toward the 53 EGFR-paralogues ($Y = 1$, if $K_D < 3$ μM).[8] The null hypothesis is the assumption that there is no correlation between the responding variable and the explanatory variables.[45,46]

Dehydron Identification. Dehydrons may be readily identified from atomic coordinates of proteins with reported structure. Thus, we first identify all intramolecular backbone hydrogen bonds within the structure as bonds whose N−O distances are <3.5 Å and N−H−O angles are >110°. For each hydrogen bond identified, we then calculate its extent of wrapping, ρ, by quantifying the number of the side chain carbonaceous nonpolar groups contained within a "dehydration domain" around such bond. This domain is

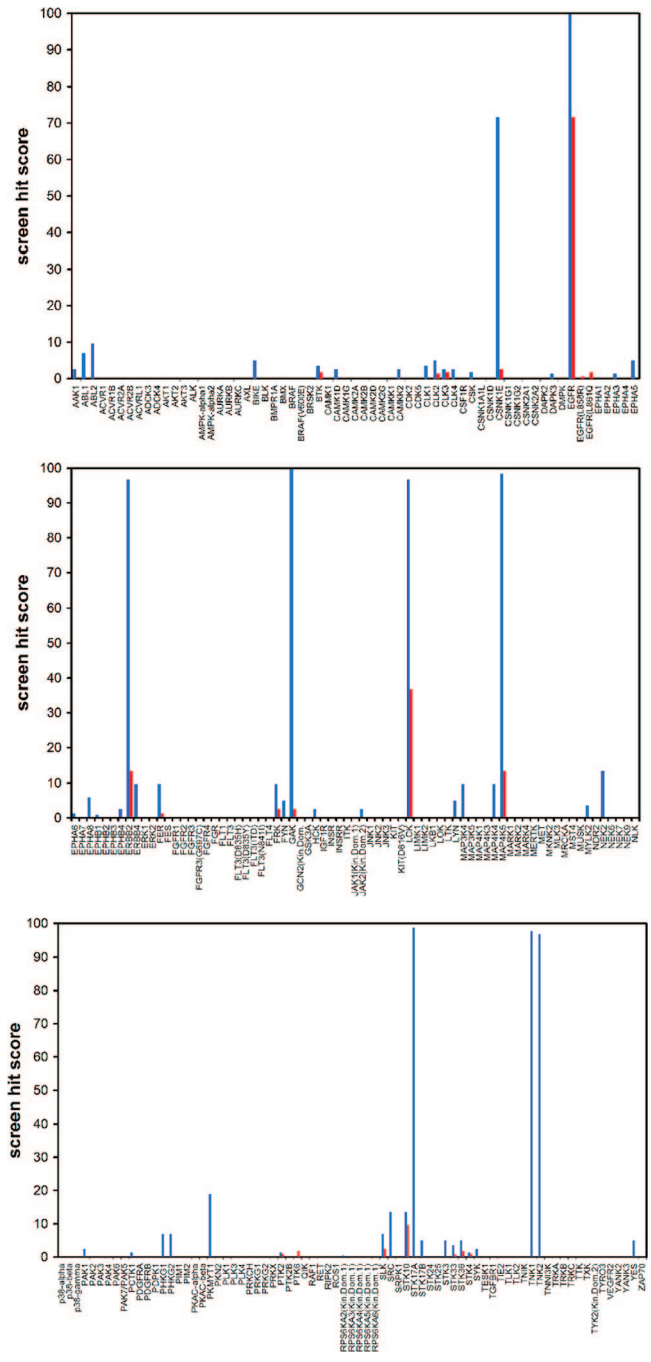

Figure 7. Affinity profile of compound **10**. High-throughput screening at 10 μM of **10** (red) over a battery of 220 human kinases displayed in a T7-bacteriophage-expressing library (Ambit Bioscience, San Diego, CA). The screening assay of **8** (blue) was used as control.[8,9] Hit values are reported as percentage bound kinase.

defined as two intersecting balls of fixed radius (~thickness of three water layers) centered at the α-carbons of the residues paired by the hydrogen bond.

In structures of soluble proteins, at least two-thirds of the backbone hydrogen bonds are wrapped on average by $\rho = 26.6 \pm 7.5$ nonpolar groups for a dehydration ball of radius 6.2 Å. Dehydrons lie in the tails of the distribution, i.e., their dehydration domains contain 19 or fewer nonpolar groups, so their ρ-values are below the mean ($\rho = 26.6$) minus one standard deviation ($\sigma = 7.5$).[23–27] Dehydrons were directly determined from a PDB file using the program YAPView (University of Chicago).[47]

Synthesis of Redesigned Compounds. (Pyrrol N6)-methyl-staurosporine (9). The synthesis of **9**[31,33,37] involves replacing the imide hydrogen atom in the pyrrol ring of staurosporine with a methyl group, as previously reported.[33] This modification was achieved by following the short pathway based on intramolecular Diels−Alder reaction of pyrano[4,3-*b*]indol-3-one, described in ref 37, page 4399, replacing the first step by treatment of commercial 2-nitrocinnamaldehyde with 1,2-dimethyl hydrazine (for pyrrol N6 methylation) instead of hydrazine. The synthesis and spectroscopic characterization of **9** is provided as Supporting Information.

4-Dimethylamino-butanoic-acid-[4-(5-chloro-4-fluoro-3-methylphenylamino)-3-methyl-7-methoxy-quinoline-6-yl]-amide (10). The synthesis of **10** entails several chemical modifications of the parental compound **8**:[32] replacing the double bond (Michael acceptor) in the acryl group with a single bond, replacing the cyanide group with a methyl, and appending a methyl group at position 3 of the terminal benzene ring. Thus, **10** was synthesized by following a pathway that recapitulates the synthesis of **8**, albeit with different reactants (Scheme 4).[32] The synthesis and spectroscopic characterization of **10** is provided as Supporting Information.

High-Throughput Screening Assay. A high-throughput screening assay of compounds **9** and **10** at 10 μM were conducted (Ambit Biosciences, San Diego, CA) against a bacteriophage library displaying 220 human kinases. The screening assays of both parental compounds (staurosporine and **8**, respectively) were used as control.[8,9] A rough estimation of the binding constant (K_d^{-1}) for each assay was provided by the single-hit value in the primary screen at a single compound concentration. Kinase profiling was performed using a bacteriophage library displaying fused human kinases that may attach at the ATP site to a fixed-ligand matrix that may be competitively displaced from binding by the tested compound.[8,9]

Acknowledgment. This research is supported by NIH grant R01-GM072614 and by an unrestricted grant from Eli Lilly. We thank Drs. Harry Harlow and Chen Su (Eli Lilly) for their valuable input.

Supporting Information Available: Wrapping comparison, predicted affinity profile, and experimental screening of **9** against 56 PDB-reported kinase structures (Methods). Synthesis and spectroscopic characterization of compounds **9** and **10**. This material is available free of charge via the Internet at http://pubs.acs.org.

References

(1) Gibbs, J.; Oliff, A. Pharmaceutical research in molecular oncology. *Cell* **1994**, *79*, 193–198.
(2) Levitski, A.; Gazit, A. Tyrosine kinase inhibition: an approach to drug development. *Science* **1995**, *267*, 1782–1788.
(3) Donato, N. J.; Talpaz, M. Clinical use of tyrosine kinase inhibitors: therapy for chronic myelogenous leukemia and other cancers. *Clin. Cancer Res.* **2000**, *6*, 2965–2966.
(4) Dancey, J.; Sausville, E. A. Issues and progress with protein kinase inhibitors for cancer treatment. *Nat. Rev. Drug Discovery* **2003**, *2*, 296–313.
(5) Tibes, R.; Trent, J.; Kurzrock, R. Tyrosine kinase inhibitors and the dawn of molecular cancer therapeutics. *Annu. Rev. Pharmacol. Toxicol.* **2005**, *45*, 357–384.
(6) Chen, J.; Zhang, X.; Fernández, A. Molecular basis for specificity in the druggable kinome: sequence-based analysis. *Bioinformatics* **2007**, *23*, 563–572.
(7) Knight, Z. A.; Shokat, K. M. Features of selective kinase inhibitors. *Chem. Biol.* **2005**, *12*, 621–637.
(8) Fabian, M. A.; Biggs, W. A.; Treiber, D. K.; Atteridge, C. E.; Azimioara, M. D.; Benedetti, M. G.; Carter, T.; Ciceri, P.; Edeen, P. T.; Floyd, M.; Ford, J. M.; Galvin, M.; Gerlach, J. L.; Grotzfeld, R. M.; Herrgand, S.; Insko, D. E.; Insko, M. A.; Lai, A.; Lélias, J. M.; Mehta, S.; Milanov, Z. V.; Velasco, A. M.; Wodicka, L. M.; Patel, H. K.; Zirrankar, P. P.; Lockhart, D. A. A small molecule-kinase interaction map for clinical kinase inhibitors. *Nat. Biotechnol.* **2005**, *23*, 329–336.
(9) Karaman, M. K.; Herrgard, S.; Treiber, D. K.; Gallant, P.; Atteridge, C. E.; Campbell, B. T.; Chan, K. W.; Ciceri, P.; Davis, M. I.; Edeen, P. T.; Faraoni, R.; Floyd, M.; Hunt, J. P.; Lockhart, D. J.; Milanov, Z. V.; Morrison, M. J.; Pallares, G.; Patel, H. K.; Pritchard, S.; Wodicka, L. M.; Zarrinkar, P. P. A quantitative analysis of kinase inhibitor selectivity. *Nat. Biotechnol.* **2008**, *26*, 127–132.

(10) Druker, B. J. Molecularly targeted therapy: have floodgates opened. *Oncologist* **2004**, *9*, 357–360.
(11) Kerkelä, R.; Grazette, L.; Yacobi, R.; Iliescu, C.; Patten, R.; Beahm, C.; Walters, B.; Shevtsov, S.; Pesant, S.; Clubb, F. J.; Rosenzweig, A.; Salomon, R. N.; Van Etten, R. A.; Alroy, J.; Durand, J.; Force, T. Cardiotoxicity of the cancer therapeutic agent imatinib mesylate. *Nat. Med.* **2006**, *12*, 908–916.
(12) Force, T.; Krause, D. S.; Van Etten, R. A. Molecular mechanisms of cardiotoxicity of tyrosine kinase inhibition. *Nat. Rev. Cancer* **2007**, *7*, 332–344.
(13) Capdeville, R.; Buchdunger, E.; Zimmermann, J.; Matter, A. Glivec (STI571, imatinib), a rationally developed, targeted anticancer drug. *Nat. Rev. Drug Discovery* **2002**, *1*, 493–502.
(14) Atkins, M.; Jones, C. A.; Kirkpatrick, P. Sunitinib maleate. *Nat. Rev. Drug Discovery* **2006**, *5*, 279–280.
(15) Rini, B. I. Sorafenib. *Expert Opin. Pharmacother.* **2006**, *7*, 453–461.
(16) McIntyre, J. A.; Er, J.; Bayes, M. Dasatinib. Treatment of leukemia treatment of solid tumors Bcr-Abl and Src kinase inhibitor. *Drugs Future* **2006**, *31*, 291–303.
(17) Leighl, N. B.; Res, D. Erlotinib: Profile report. *Drugs Ther. Perspect.* **2006**, *22*, 1–2.
(18) Cappuzzo, F.; Finocchiaro, G.; Metro, G.; Bartolini, S.; Magrini, E.; Cancellieri, A.; Trisolini, R.; Castaldini, L.; Tallini, G.; Crino, L. Clinical experience with gefitinib: An update. *CRC Crit. Rev. Oncol. Hematol.* **2006**, *58*, 31–45.
(19) Fernández, A.; Sanguino, A.; Peng, Z.; Ozturk, E.; Chen, J.; Crespo, A.; Wulf, S.; Shavrin, A.; Qin, C.; Ma, J.; Trent, J.; Lin, Y.; Han, H.; Mangala, L. S.; Bankson, J. A.; Gelovani, J.; Samarel, A.; Bornmann, W.; Sood, A. K.; López-Berestein, G. An anticancer C-kit kinase inhibitor is re-engineered to make it more active and less cardiotoxic. *J. Clin. Invest.* **2007**, *117*, 4044–4054.
(20) Demetri, G. Structural reengineering of imatinib to decrease cardiac risk in cancer therapy. *J. Clin. Invest.* **2007**, *117*, 3650–3653.
(21) Crunkhorn, S. Anticancer drugs: Redesigning kinase inhibitors. *Nat. Rev. Drug Discovery* **2008**, *7*, 120–121.
(22) Crespo, A.; Fernández, A. Kinase packing defects as drug targets. *Drug Discovery Today* **2007**, *12*, 917–923.
(23) Fernández, A.; Scheraga, H. A. Insufficiently dehydrated hydrogen bonds as determinants of protein interactions. *Proc. Natl. Acad. Sci. U.S.A.* **2003**, *100*, 113–118.
(24) Fernández, A.; Scott, L. R. Adherence of packing defects in soluble proteins. *Phys. Rev. Lett.* **2003**, *91*, 018102.
(25) Fernández, A.; Scott, L. R. Dehydron: A structurally encoded signal for protein interaction. *Biophys. J.* **2003**, *85*, 1914–1928.
(26) Fernández, A. Keeping dry and crossing membranes. *Nat. Biotechnol.* **2004**, *22*, 1081–1084.
(27) Pietrosemoli, N.; Crespo, A.; Fernández, A. Dehydration propensity of order−disorder intermediate regions in soluble proteins. *J. Proteome Res.* **2007**, *6*, 3519–3526.
(28) Fernández, A. Incomplete protein packing as a selectivity filter in drug design. *Structure* **2005**, *13*, 1829–1836.
(29) Fernández, A.; Sanguino, A.; Peng, Z.; Crespo, A.; Ozturk, E.; Zhang, X.; Wang, S.; Bornmann, W.; López-Berestein, G. Rational drug redesign to overcome drug resistance in cancer therapy: imatinib moving target. *Cancer Res.* **2007**, *67*, 4028–4033.
(30) Fernández, A.; Berry, R. S. Molecular dimension explored in evolution to promote proteomic complexity. *Proc. Natl. Acad. Sci. U.S.A.* **2004**, *101*, 13460–13465.
(31) Link, J. T.; Raghavan, S.; Danishefsky, S. J. First total synthesis of staurosporine and ent-staurosporine. *J. Am. Chem. Soc.* **1995**, *117*, 552–553.
(32) Wissner, A.; Overbeek, E.; Reich, M. F.; Floyd, M. B.; Johnson, B. D.; Mamuya, N.; Rosfjord, E. C.; Discafani, C.; Davis, R.; Shi, X.; Rabindran, S. K.; Gruber, B. C.; Ye, F.; Hallett, W. A.; Nilakantan, R.; Shen, R.; Wang, Y.; Greenberger, L. M.; Tsou, H. Synthesis and structure−activity relationships of 6,7-disubstituted 4-anilinoquinoline-3-carbonitriles. The design of an orally active, irreversible inhibitor of the tyrosine kinase activity of the epidermal growth factor receptor (EGFR) and the human epidermal growth factor receptor-2 (HER-2). *J. Med. Chem.* **2003**, *46*, 49–63.
(33) Fernández, A.; Maddipati, S. The a priori inference of cross reactivity for drug-targeted kinases. *J. Med. Chem.* **2006**, *49*, 3092–3100.
(34) Zhao, B.; Bower, M. J.; McDevitt, P. J.; Zhao, H.; Davis, S. T.; Johanson, K. O.; Green, S. M.; Concha, N. O.; Zhoud, B. S. Structural basis for Chk1 inhibition by UCN-01. *J. Biol. Chem.* **2002**, *277*, 46609–46615.
(35) Atwell, S.; Adams, J. M.; Badger, J.; Buchanan, M. D.; Feil, I. K.; Froning, K. J.; Gao, X.; Hendle, J.; Keegan, K.; Leon, B. C.; Müller-Dieckmann, H. J.; Nienaber, V. L.; Noland, B. W.; Post, K.; Rajashankar, K. R.; Ramos, A.; Russell, M.; Burley, S. K.; Buchanan, S. G. Novel mode of Gleevec binding is revealed by the structure of Spleen Tyrosine Kinase. *J. Biol. Chem.* **2004**, *279*, 55827–55832.
(36) Sanner, M. F.; Olson, A. J.; Spehner, J. C. Reduced surface: An efficient way to compute molecular surfaces. *Biopolymers* **1996**, *38*, 305–320.
(37) Knölker, H. J.; Reddy, K. R. Isolation and synthesis of biologically active carbazole alkaloids. *Chem. Rev.* **2002**, *102*, 4303–4427.
(38) Demetri, G. D.; von Mehren, M.; Blanke, C. D.; Van den Abbeele, A. D.; Eisenberg, B.; Roberts, P. J.; Heinrich, M. C.; Tuveson, D. A.; Singer, S.; Janicek, M.; Fletcher, J. A.; Silverman, S. G.; Silberman, S. L.; Capdeville, R.; Kiese, B.; Peng, B.; Dimitrijevic, S.; Druker, B. J.; Corless, C.; Fletcher, C. D. M.; Joensuu, H. Efficacy and safety of imatinib mesylate in advanced gastrointestinal stromal tumors. *N. Engl. J. Med* **2002**, *347*, 472–480.
(39) Halder, J. B.; Lin, Y. G.; Merritt, W. M.; Spannuth, W. A.; Nick, A. M.; Honda, T.; Kamat, A. A.; Han, L.; Kim, T. J.; Lu, C.; Tari, A. M.; Bornmann, W.; Fernández, A.; López-Berestein, G.; Sood, A. K. Therapeutic efficacy of a novel FAK inhibitor TAE226 in ovarian carcinoma. *Cancer Res.* **2007**, *67*, 10976–10983.
(40) Hauck, C. R.; Hsia, D. A.; Puente, X. S.; Cheresh, D. A.; Schlaepfer, D. D. FRNK blocks v-Src stimulated invasion and experimental metastasis without effects on cell motility or growth. *EMBO J.* **2002**, *21*, 6289–6302.
(41) Torrance, C. J.; Jackson, P. E.; Montgomery, E.; Kinzler, K. W.; Vogelstein, B.; Wissner, A.; Nunes, M.; Frost, P.; Discafani, C. M. Combinatorial chemoprevention of intestinal neoplasia. *Nat. Med.* **2000**, *6*, 1024–1028.
(42) Erlichman, C.; Hidalgo, M.; Boni, J. P.; Martins, P.; Quinn, S. E.; Zacharchuk, C.; Amorusi, P.; Adjei, A. A.; Rowinsky, E. K. Phase I study of EKB-569, an irreversible inhibitor of the epidermal growth factor receptor, in patients with advanced solid tumors. *J. Clin. Oncol.* **2006**, *24*, 2252–2260.
(43) Holm, L.; Park, J. DaliLite workbench for protein structure comparison. *Bioinformatics* **2000**, *16*, 566–567.
(44) DaliLite Pairwise Comparison of Protein Structures. http://www.ebi-.ac.uk/DaliLite/ (accessed May 2008).
(45) Agresti, A. *Logistic Regression. An Introduction to Categorical Data Analysis.* Wiley Interscience: New York, 1996; pp 103−144.
(46) Logistic Regression. http://statpages.org/logistic.html (accessed May 2008).
(47) Protein Library. http://protlib.uchicago.edu/dloads.html (accessed May 2008).

JM800453A